Silikáty 29, s. 193—202 (1985)

Původní práce

FORMATION OF CONVECTIVE FLOW IN GLASS MELTS DUE TO VAPORIZATION OF A SURFACE ACTIVE COMPONENT

PART I: Experimental method and results

Lubomír Němec, Ivo Bařtipán*)

Joint Laboratory for the Chemistry and Technology of Silicates
Czechoslovak Academy of Sciences and Institute of Chemical Technology
Suchbátarova 5, 166 28 Prague 6
*) *Sklo Union, Concern Corporation, Sklotas, Dukla Oloví Works*

Received 9. 10. 1984

In the vaporization of fluorides from opal glass melts and in that of boron oxide from Neutral glass there occurs the so-called cell flow which is caused by surface forces. Application of the high-temperature motion-picture technique permitted the shape and the rate of this flow to be determined at 1250—1350 °C in the atmosphere of flowing dry and moist nitrogen. The rates of flow determined were of an order of 10^{-5} to 10^{-4} m s^{-1} and their courses in terms of time were in qualitative agreement with the volatilization losses of fluorides from the glass melt.

INTRODUCTION

Volatilization of some glass components into the atmosphere is responsible for losses in valuable raw materials, for impairing the quality of glass, damaging the melting plant and for adverse effcts on the living environment. This is why this phenomenon has been the subject of extensive studies in recent years. With respect to the conditions of volatilization, most attention is paid to lead, borosilicate and fluoride glasses. The volatilization mechanism includes the transport of the volatile component through the glass melt, its transition through the phase boundary and its transport as a gaseous phase. Any of these processes can be the controlling process of the transport according to the respective conditions. Diffusion transport in liquid phase [1, 2] was usually regarded as the slowest, i. e. the control process of volatilization; however, it was later found that convection caused by gravity or surface forces arising as a result of concentration fluctuations of the evaporating substance, may play a significant role in the transport. In that case, transport through the phase boundary or the gaseous phase [3, 4] may be the control process, because the convective transfer in the glass melt will significantly speed up the transport of the volatile substance to the phase boundary. The term cell flow has been derived from the shape of the small practically closed formation of convective streams at the surface; however, there has so far not been direct evidence for their existence in glass melts.

The present study had the aim to provide this evidence for lead, fluoride and borosilicate glass melts, to find correlation between such flow and the vaporization rate for fluoride glass melts, to suggest the vaporization model which would comply with the experimental conditions, and to establish a correlation between this model and the course of vaporization in industrial furnaces. The first part will present a description of the measuring method, the equipment, and the experimental results. The second part is an analysis of the results, a design and derivation of the vaporization model.

SELECTION AND DESCRIPTION OF THE EXPERIMENTAL METHOD

The convective contribution arises above all as a result of the difference between the mass densities at various points of the glass melt, and possibly under the effect of a surface tension gradient. The latter case is of interest with the glass melts in question. Vaporization of the surface active component brings about a decrease of its concentration in the melt at the boundary, and an increase in interphase energy. Any fluctuation which brings to the surface liquid with a lower surface tension leads to spreading of this fresh liquid over the phase boundary and to the formation of cell flow at the surface. Additions of fluorides, B_2O_3 or PbO are known to reduce the surface tension of glass melts. It may therefore be expected that the influence of the surface forces can be effected in the process of their vaporization.

The motion-picture technique was chosen to provide evidence for the existence of cell flow in the glass melts. The method has already been described in detail in an earlier study [5], so that just the functions relating to the motion-picture recording of the cell flow will be dealt with. Experimental evidence requires that the flow of liquid in the measuring cell be rendered visible. Colouring of the glass melt with cobalt nitrate, introduction of powdered corundum, sand, powdered zirconium dioxide and microscopic bubbles were used. The microscopic bubbles were the only successful flow indicator. Owing to their small dimensions, their movement described well the shape of flow in the melt. A movie camera provided with a stepped motor was used to record the flow. To improve the recording of the flow in some instances, the glass melt was coloured with cobalt nitrate crystals and the specimens were subject to visual and photographic evaluation after cooling down. Supplementary information was provided by pycnometric determination of density and by chemical determination of fluorides and Na_2O in the glasses (State Glass Research Institute at Hradec Králové).

A schematic diagram of the motion picture apparatus is shown in Fig. 1. The measuring cells employed were silica glass. The cells were observed from the side, with the exception of one case from the top. Dry or moist nitrogen was passed over the glass melt surface to produce a defined atmosphere and to remove the volatilized substances.

The flow was mostly studied on an opal—triplex glass melted in pot furnaces, on lead crystal containing 24 wt. % PbO, and on the Neutral borosilicate glass. The temperature exposures were from 1 to 24 hours; the shape intensity of flow were followed at 1250, 1300, 1350 and 1400 °C; the rate of flow of nitrogen above the surface was in the range of 1.67×10^{-6} m^3 s^{-1} to 8.33×10^{-6} m^3 s^{-1} under normal conditions; the partial water vapour pressures in nitrogen amounted to 0, 0.5 and 30 kPa. The rate of motion-picture taking was in the range of 1 picture per second to 0.045 picture per second.

The rate of flow was determined by measuring the path and time of the moving bubbles during the screenings of the films obtained. Following correction for magnification, the screening rate and exposure, the actual rate of flow was calculated. The mean rate of flow in the "cells" and the so-called surface rates of flow (the mean rates of flow of the melt in horizontal direction in close proximity of the surface) were determined.

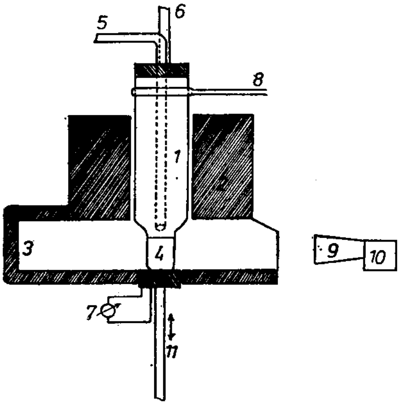

Fig. 1. Schematic diagram of the apparatus for lateral observation and motion-picture recording of melts;
1 — silica glass cell, 2 — resistance chamber furnace, 3 — black body, 4 — melted glass, 5 — atmosphere inlet, 6 — atmosphere outlet, 7 — thermocouple, 8 — holder, 9 — teleobjective, 10 — movie camera with a timing unit, 11 — travel (feed).

The shape of flow was also established by means of spherical silica glass test tubes or corundum crucibles with a planar bottom. The glass melt was coloured with cobalt nitrate and exposed at the given temperature in the furnace. Following cooling down, the specimens with the coloured striae formed by flow were photographed from the top or in a cross section perpendicular to the surface.

EXPERIMENTAL RESULTS

The shape of the flow could be observed only after screening the developed films; the process studied could thus be speeded up 24 to 528 times as required. All the films proved explicitly that at the respective temperatures, the borosilicate and particularly fluoride glass melts showed various types of flow, whose shapes are shown schematically in Fig. 2. One type of flow tended to change into another in the course of a single measurement. Fig. 3 shows a photograph of the bottom

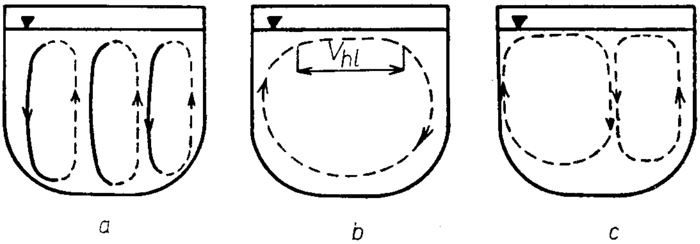

Fig. 2. Schematic diagram of various types of flow observed in the measuring cell.

part of the cell at the melting temperatures. The photograph was taken from the screen, using a suitably long exposure allowing to obtain an approximate pattern of the flow, which was otherwise well discernible during the motion picture screening. The main evidence of the shape and rates of flow is provided by the films that can be made available by the present authors.

However, it was also necessary to prove that the flow is actually the result of the effect of surface forces and not one of temperature convection due to inhomogeneity of the temperature field in the specimen. This is why the supply of nitrogen was turned off in several of the experiments. After a certain period of time, the atmosphere above the glass melt becomes saturated with the products of volatilization and this stops. Experiments have proved that convective flow stops almost immediately after turning off the supply of gases and the indicating bubbles start to rise towards the surface. The flow therefore occurs as a consequence of evaporation; however, supplementary measurements have to be carried out to estimate a possible effect of density convection on the flow.

The shape of the rotary cells on the melt surface was investigated by studying cooled specimens of the fluoride glass coloured with cobalt nitrate. Fig. 4 demonstrates quite well the shape of cell flow at the melt surface occurring in the melting of fluoride glass in a quartz cell and in air atmosphere. The shape of the flow with approximately radial boundaries, arising in the melting of the same glass in a cylindrical corundum crucible, is shown in Fig. 5, whereas Fig. 6 illustrates the shape of convective flow over the fracture surface of the specimen roughly perpendicular to the surface. As indicated by Fig. 7, even two-hour thermal exposure at 1300 °C failed to provide explicit evidence on the formation of cell flow in lead glass melt. The decolorized glass melt was agitated at the surface only and the possibly arising convective flow can be assumed to have a small vertical range only as a result of the density stabilization of lead glass with respect to flow in the course of vaporization.

Further measurements were carried out to determine the mean rates of flow in the cell, v_{pr}, and the surface flow rate, v_{hl}, under the conditions specified in the paragraphs above. The place where the surface rates of flow were scanned, is shown in Fig. 2b. Results are plotted in Figs. 8 through 12 in the form of a time dependence of the rate of flow. In all the instances, the measurements were carried out in flowing dry nitrogen atmosphere; the first numerical value in brackets in the figure captions specifies the partial pressure of water vapour in nitrogen, in kPa. The points shown in Fig. 8 through 12 are the mean values of the rates of flow during an average time. Each value of the time of measurement is the mean value of a time interval of about 20 minutes. The maximum relative error due to vaveraging in the initial region (up to 1 hour) amounts to 25 %, as related to the mean rate of flow during the average time. Between the first and the fifth hour, the maximum relative error amounts to 12 %, and to 5 % at the end of the measurement.

The pycnometric measurements of glass density had the purpose to show if density convection may have taken part in the flow. The densities were determined by the four-pycnometr method on the following basic glasses:
1 — basic opal glass
3 — opal glass bubbled through with nitrogen and water vapour with a partial pressure of 0.5 kPa at 1300 °C
2 — opal glass bubbled through with saturated steam at 1300 °C (a decrease of fluorides content from 5.3 % down to 1.3 %).

The density values are listed in Table I. Glass No. 2 shows a slightly higher density and glass No. 3 a density a little lower than that of the base glass. As the flow intensity in the case of the drier nitrogen was always higher than in the case of moist nitrogen (cf. Figs. 8 through 12), the density convection does not clearly take any part in the formation of the flow.

Table I

Densities of opal glasses, measured pycnometrically

Glass No.	Values measured $\varrho/\text{kg m}^{-3}/\times 10^{-3}$	Mean values $\varrho/\text{kg m}^{-3}/\times 10^{-3}$
1	2.4290 2.4314	2.430
2	2.4441 2.4500	2.447
3	2.4255 2.4267	2.426

A number of opal glass specimens were analyzed for the concentration of Na_2O and fluorides to determine the time loss of the volatile substance and the proportion of the volatile components. The determination was carried out at the State Glass Research Institute at Hradec Králové. A plot of the results obtained at 1300 °C is shown in Fig. 13. The time course of the loss of fluorides and Na_2O is in a qualitative agreement with the decrease of the rate of flow (cf. Fig. 9).

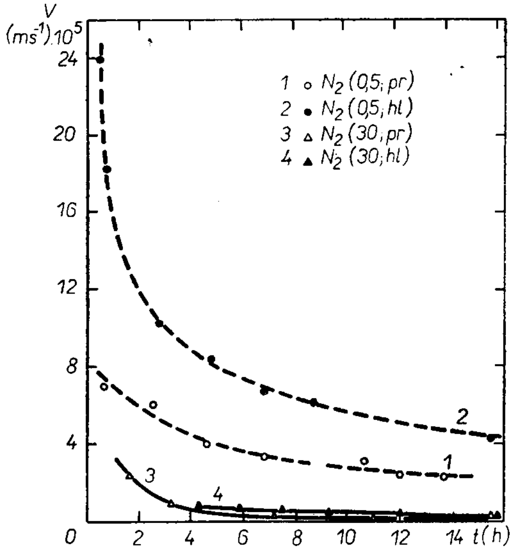

Fig. 8. Time dependence of the rate of flow of fluoride glass melt, 1250 °C, rate of flow of gases 1.67×10^{-6} $m^3 s^{-1}$ under normal conditions. The numerals 0.5 and 30 in the diagrams (also in the following ones) indicate the partial pressure of water vapour in kPa.

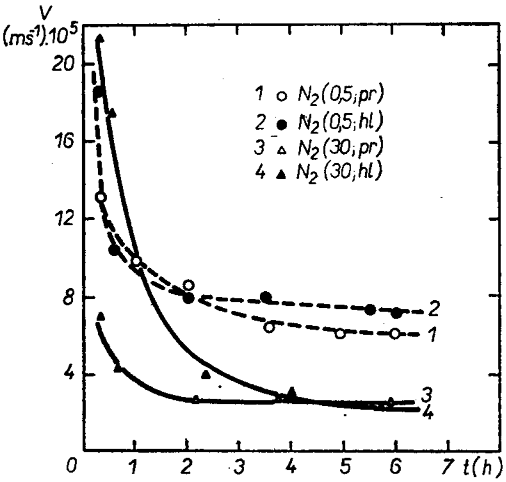

Fig. 9. Time dependence of the rate of flow of fluoride glass melt, 1300 °C, rate of flow of gases 1.67 × 10^{-6} m³ s⁻¹ under normal conditions.

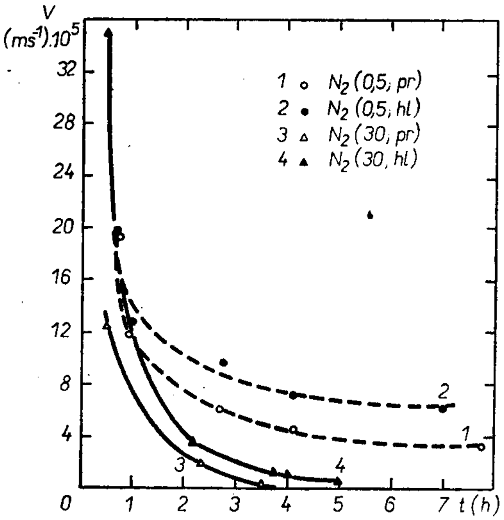

Fig. 10. Time dependence of the rate of flow of fluoride glass melt. 1350 °C, rate of flow of gases 1.67 × 10^{-6} m³ s⁻¹ under normal conditions.

A BRIEF SUMMARY OF THE EXPERIMENTAL RESULTS

The motion-picture films have safely proved the existence of cell flow in opal glass melts and in borosilicate glass melts. The results indicate that in a measuring cell there always occur several rotating formations whose characteristics remain unchanged for a longer period of time; however, both the direction of flow and its distribution often underwent a change in the course of the measurement. It is probable that in the first stages of measurement the liquid at the surface would flow in particular against the direction of the flowing glass, so that a descending flow would be formed at the point where fresh gas meets the melt surface (the lowest concentration of the surface active substance). Such an arrangement is indicative of convective flow resulting from differences in surface tension. Density measurements on glasses with considerably differing fluoride contents showed

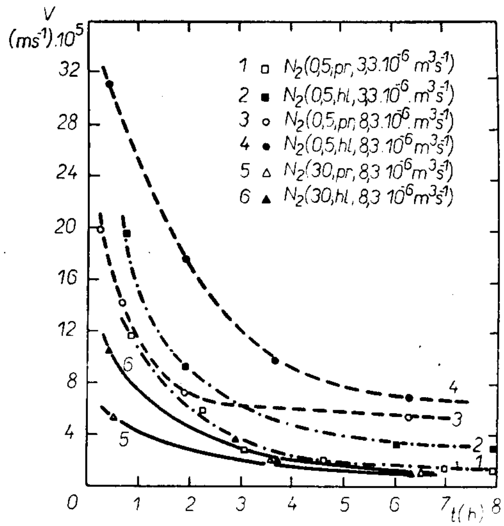

***Fig. 11.** Time dependence of the rate of flow of fluoride glass melt, 1300 °C, rate of flow of gases 3.3×10^{-6} and 8.3×10^{-6} m^3 s^{-1} under normal conditions.*

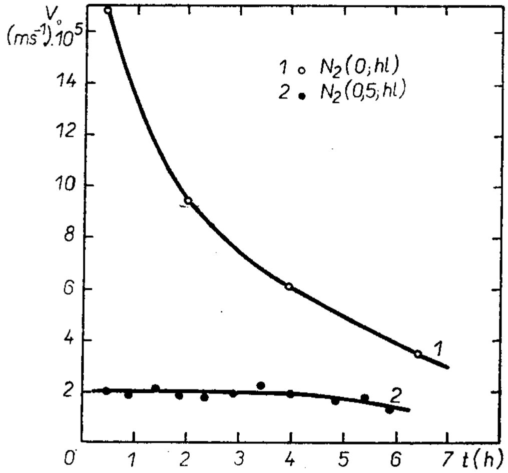

***Fig. 12.** Time dependence of the rate of flow of fluoride glass melt (1) and Neutral glass melt (2), 1300 °C, rate of flow of gases 1.67 $\times$ 10^{-6} m^3 s^{-1} under normal conditions.*

that density convection has no share in the formation of cell flow. Experiments with turned-off flow of the atmosphere ruled out participation of thermic convection in the volatilization. Similarly, cell flow was observed in the borosilicate glass melt, and is likely to affect the mechanism and intensity of volatilization of B_2O_3 from these glasses.

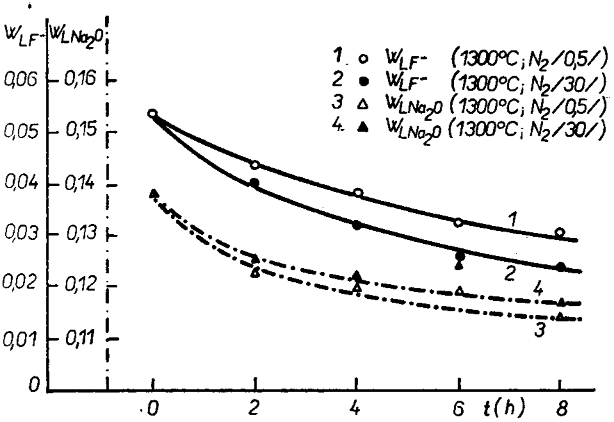

Fig. 13. Time dependence of the content of sodium fluorides and oxides in fluoride glass melt; w_{LF} *— weight fraction of fluorides in liquid phase,* w_{LNa_2O} *— weight fraction of* Na_2O *in liquid phase.*

No firm evidence was found for the formation of cell flow in lead glass melts. Direct observation of the melt is impossible owing to the intransparency of lead glass melts; study of the cooled specimens of lead glass coloured with cobalt nitrate indicated that the expected convection [6] is only effective in a thin layer at the surface as a result of the density stabilization of the melt.

The experimental arrangement represents a system with a well mixed atmosphere above the surface, and thus roughly corresponds to industrial furnaces with free melt surfaces heated from the top. The results obtained may therefore be technologically significant. The second part of the present study will deal in more detail with the results including the degrees of hydrolysis of the volatilizing fluorides, evaluation of the effect of experimental conditions on the rate of convective flow and the approximate mathematical model describing the mechanism of the volatilization of fluorides. This model will be used in quantitative evaluation of the course of vaporization of fluorides from an opal glass melt.

References

[1] Preston E., Turner W. E. S.: Jour. Soc. Glass Technol. *16*, 331 (1932), ibid. *19*, 296 (1935).
[2] Oldfield L. F., Wright R. D.: Glass Technol. *3*, 59 (1962).
[3] Grosman P., Matoušek J., Hlaváč J.: Paper of the Institute of Technology *16*, 177 (1975).
[4] Matoušek J., Hlaváč J.: Glass Technol. *12*, 103, (1971).
[5] Žlutický J., Němec L.: Glastechn. Ber. *50*, 59 (1977).
[6] Heřmánková A.: Thesis, Dept. of the Technology of Silicates, Institute of Chemical Technology, Prague (1980).

VZNIK KONVEKTIVNÍHO PROUDĚNÍ VE SKLOVINÁCH PŘI VYPAŘOVÁNÍ POVRCHOVĚ AKTIVNÍ SLOŽKY

I. EXPERIMENTÁLNÍ METODA A VÝSLEDKY MĚŘENÍ

Lubomír Němec, Ivo Bařtipán*)

Společná laboratoř pro chemii a technologii silikátů ČSAV a VŠCHT
166 28 Praha 6
*) *Sklo Union, koncernový podnik, Sklotas, závod Dukla Oloví*

Při tavení skla dochází k nežádoucímu vypařování některých složek sklovin. Metodou filmování za vysokých teplot bylo zkoumáno chování skloviny obsahující fluoridy (opál), oxid boritý (Neutral) a oxid olovnatý (křišťál) při vypařování těchto složek. Sledování ukázala, že u fluoridové a borité skloviny dochází při vypařování těkavých povrchově aktivních složek ke vzniku tzv. buňkového proudění, které způsobují povrchové síly. U olovnaté skloviny se toto proudění nepodařilo jednoznačně prokázat. Při vyhodnocení filmů získaných při teplotách 1250—1400 °C se podařilo získat tvary proudění a přibližné rychlosti proudění, které se pohybují v hodnotách řádově 10^{-5}—10^{-4} m . s^{-1}, což zhruba odpovídá rychlosti proudění způsobeného teplotními gradienty v průmyslové tavicí peci. Výsledky jsou podkladem pro navržení matematického modelu vypařování těkající povrchově aktivní látky.

Obr. 1. Schéma aparatury pro boční pozorování a filmování taveniny;
1 — křemenná kyveta, 2 — odporová komorová pec, 3 — černé těleso, 4 — roztavená sklovina, 5 — přívod atmosféry, 6 — odvod atmosféry, 7 — termočlánek, 8 — držák, 9 — teleobjektiv, 10 — kamera s časovou jednotkou, 11 — posuv.

Obr. 2. Schematický tvar různých typů proudění pozorovaných v měřicí kyvetě.

Obr. 3. Tvar proudění v měřicí kyvetě získaný fotografováním z plátna s dlouhou expozicí. Fluoridová sklovina, 1300°C.

Obr. 4. Tvar proudových buněk fluoridové skloviny na hladině ve filmovací křemenné kyvetě, teplota 1300 °C, tepelná expozice 4h, vzduchová otevřená atmosféra.

Obr. 5. Tvar proudových buněk fluoridové skloviny na hladině při tavení v korundovém kelímku, teplota 1300 °C, tepelná expozice 2h, vzduchová otevřená atmosféra.

Obr. 6. Tvar proudové buňky fluoridové skloviny v lomu vzorkem zhruba kolmém k hladině, teplota 1400 °C, tepelná expozice 4,5 h, otevřená vzduchová atmosféra, filmovací kyveta.

Obr. 7. Obrázek kolmého řezu olovnatou sklovinou tavenou ve válcovitém korundovém kelímku a přibarvenou dusičnanem kobaltnatým, teplota 1300 °C, tepelná expozice 2h, otevřená vzduchová atmosféra.

Obr. 8. Časová závislost rychlosti proudění fluoridové skloviny, teplota 1250 °C, průtok plynů $1{,}67 \, . \, 10^{-6} \, m^3 \, s^{-1}$ *za normálních podmínek. Číslice 0,5 a 30 v obrázcích (i dalších), parciální tlak vodní páry v kPa.*

Obr. 9. Časová závislost rychlosti proudění fluoridové skloviny, teplota 1300 °C, průtok plynů $1{,}67 \, . \, 10^{-6} \, m^3 \, . \, s^{-1}$ *za normálních podmínek.*

Obr. 10. Časová závislost rychlosti proudění fluoridové skloviny, teplota 1350 °C, průtok plynů $1{,}67 \, . \, 10^{-6} \, m^3 \, . \, s^{-1}$ *za normálních podmínek.*

Obr. 11. Časová závislost rychlosti proudění fluoridové skloviny, teplota 1300 °C, průtok plynů $3{,}3 \, . \, 10^{-6}$ *a* $8{,}3 \, . \, 10^{-6} \, m^3 \, . \, s^{-1}$ *za normálních podmínek.*

Obr. 12. Časová závislost rychlosti proudění fluoridové skloviny (1) a skloviny Neutrál (2), teplota 1300 °C, průtok plynů $1{,}67 \, . \, 10^{-6} \, m^3 \, . \, s^{-1}$ *za normálních podmínek.*

Obr. 13. Závislost obsahu fluoridů a oxidů, sodného ve fluoridové sklovině na čase. w_{LF^-} *— hmotnostní zlomek fluoridů v kapalné fázi,* $w_{\mathrm{LNa_2O}}$ *— hmotnostní zlomek* Na_2O *v kapalné fázi.*

ВОЗНИКНОВЕНИЕ КОНВЕКЦИОННОГО ТЕЧЕНИЯ В СТЕКЛОМАССАХ ПРИ ИСПАРЕНИИ ПОВЕРХНОСТНО-АКТИВНОГО КОМПОНЕНТА.
I. ЭКСПЕРИМЕНТАЛЬНЫЙ МЕТОД И РЕЗУЛЬТАТЫ ИЗМЕРЕНИЯ

Лубомир Немец и Иво Барштипан*)

Общая лаборатория химии и технологии силикатов ЧСАН и ХТИ
166 28 Прага 6
*) *СКЛО-УНИОН, концерн. предприятие Склотас, завод Дукла Олови*

При варке стекла происходит нежелательное испарение некоторых компонентов стекломассы. С помощью киносъемки при высоких температурах исследовали поведение стекомассы, содержащей фториды (опал), оксид трехвалентного бора (нейтрал) и оксид двухвалентного свинца (хрусталь) при испарении приводимых компонентов. На основании исследования было доказано, что у фторидной и борной стекломасс происходит при испарении летучих поверхностно-активных компонентов так наз. клеточное течение, вызываемое поверхностными силами. В случае свинцовой стекломассы приводимое течение не удалось вполне доказать. При оценке кинопленок, полученных при температурах 1250—1400 °C были получены формы течения и приблизительные скорости течения, находящиеся в пределах величин порядка 10^{-5}—10^{-4} м . $с^{-1}$, что в общем соответствует скорости течения, вызванного температурными градиентами в промышленной плавильной печи. Полученные результаты служат основой для предложения математической модели испарения летучего поверхностно-активного вещества.

Рис. 1. *Схема аппаратуры для побочного наблюдения и киносъемки расплава; 1 — кварцевая кювета, 2 — электрическая камерная печь сопротивления, 3 — черное тело, 4 — расплавленная стекломасса, 5 — подвод атмосферы, 6 — отвод атмосферы, 7 — термоэлемент, 8 — держатель, 9 — телеобъектив, 10 — камера с единицей времени, 11 — смещение.*

Рис. 2. *Схематическая форма разных типов течения, наблюдаемых в измерительной кювете.*

Рис. 3. *Форма течения в измерительной кювете, полученная с помощью фотосъемки из экрана с длительной экспозицией. Фторидная стекломасса, 1300 °C.*

Рис. 4. *Форма клеток течения фторидной стекломассы на уровне в съемочной кварцевой кювете, температура 1300 °C, термическая экспозиция 4 часа, воздушная открытая атмосфера.*

Рис. 5. *Форма клеток течения фторидной стекломассы на уровне при плавке в корундовом тигле, температура 1300 °C, термическая экспоизиця 2 часа, воздушная открытая атмосфера.*

Рис. 6. *Форма клетки течения фторидной стекломассы в преломлении пробой, приблизительно перпендикулярном к уровню, температура 1400 °C, термическая экспозиция 4,5 ч, открытая воздушная атмосфера, съемочная кювета.*

Рис. 7. *Съемка перпендикулярного сечения свинцовой стекломассой, плавленной в цилиндрическом корундовом тигле и окрашенной нитратом двухвалентного кобальта, температура 1300 °C, термическая экспозиция 2 часа, открытая воздушная атмосфера.*

Рис. 8. *Временная зависимость скорости течения фторидной стекломассы, температура 1250 °C, проток газов 1,67 .* 10^{-6} *м*^{3} *с*$^{-1}$ *при нормальных условиях. Цифры 0,5 и 30 обозначают на рисунках парциальное давление водяного пара в кПа.*

Рис. 9. *Временная зависимость скорости течения фторидной стекломассы, температура 1300 °C, проток газов 1,67 .* 10^{-6} *м*^{3} *с*$^{-1}$ *при нормальных условиях.*

Рис. 10. *Временная зависимость скорости течения фторидной стекломассы, температура 1350°C, проток газов 1,67 .* 10^{-6} *x м*^{3}.*с*$^{-1}$ *при нормальных условиях.*

Рис. 11. *Временная зависимость скорости течения фторидной стекломассы, температура 1300 °C, проток газов 3,3 .* 10^{-6} *и 8,3 .* 10^{-6} *м*^{3} *с*$^{-1}$ *при нормальных условиях.*

Рис. 12. *Временная зависимость скорости течения фторидной стекломассы (1) и стекломассы Нейтрал (2), температура 1300 °C, проток газов 1,67 .* 10^{-6} *м*^{3} *с*$^{-1}$ *при нормальных условиях.*

Рис. 13. *Зависимость содержания фторидов и оксида натрия во фторидной стекломассе от времени;* w_{LF} *— весовая доля фторидов в жидкой фазе,* $w_{\mathrm{LNa_2O}}$ *— весовая доля* Na_2O *в жидкой фазе.*

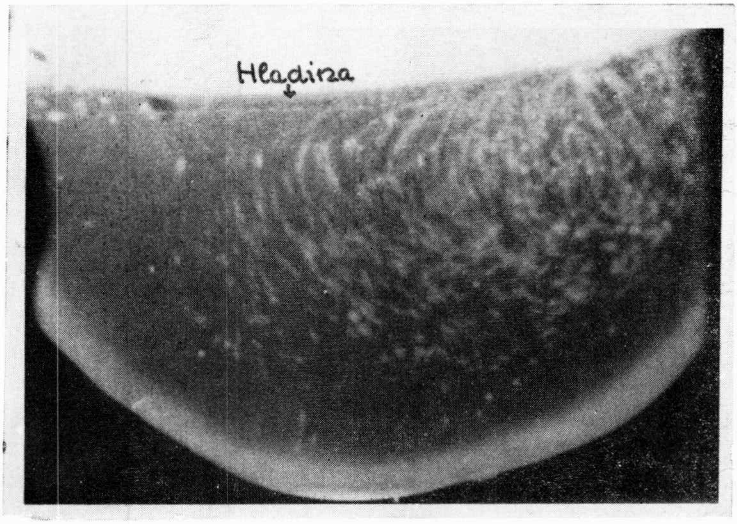

Fig. 3. The shape of flow in the measuring cell established by long exposure photography from the projecting screen. Fluoride glass melt, 1300 °C.

Fig. 4. The shape of flow cells of a fluoride glass melt on the surface in a silica glass cell, 1300 °C, thermal exposure 4 hours, air open atmosphere.

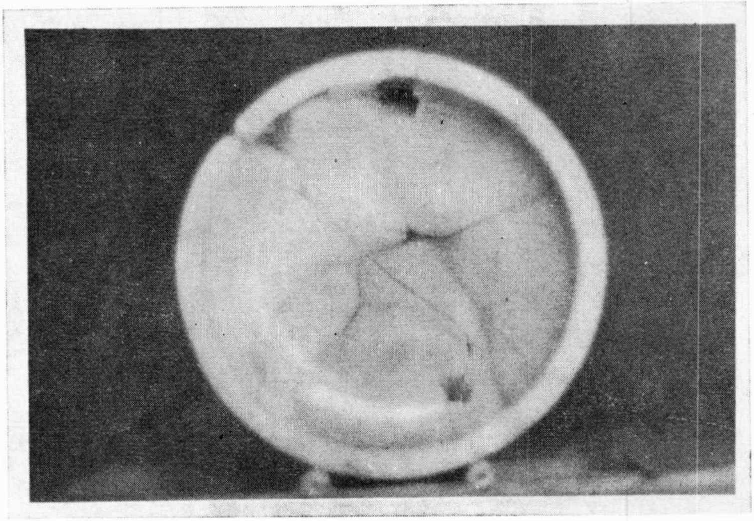

Fig. 5. The shape of flow cells of a fluoride glass melt on the surface on melting in corundum crucible, 1300 °C, thermal exposure 2 hours, air open atmosphere.

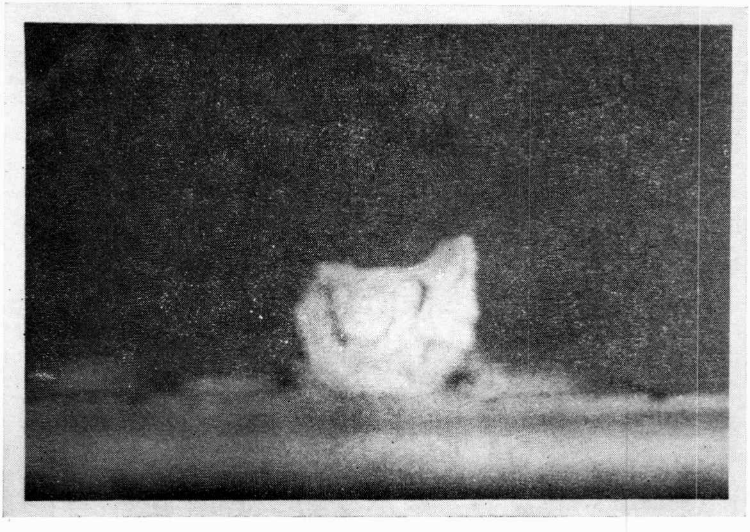

Fig. 6. The shape of a flow cell of fluoride glass melt over a fracture surface roughly perpendicular to the surface, 1400 °C, thermal exposure 4.5 hours, open air atmosphere, motion-picture cell.

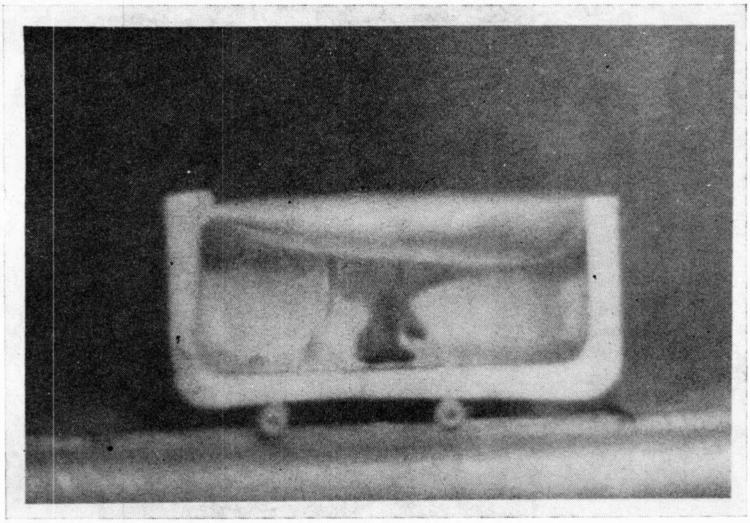

Fig. 7. Sectional view through lead glass melted in a cylindrical corundum crucible and coloured with cobalt nitrate, 1300 °C, thermal exposure 2 hours, open air atmosphere.